Supporting Information

A Three-Dimensional Lead Halide Perovskite-Related Ferroelectric

Han-Yue Zhang,[†] Xian-Jiang Song,[†] Hao Cheng,[§] Yu-Ling Zeng,[§] Yi Zhang,[†] Peng-Fei Li,[§] Wei-Qiang Liao,[§] and Ren-Gen Xiong*[,†,§]

[†]Jiangsu Key Laboratory for Science and Applications of Molecular Ferroelectrics, Southeast University, Nanjing 211189, People's Republic of China

[§]Ordered Matter Science Research Center, Nanchang University, Nanchang 330031, People's Republic of China

Corresponding Author

*xiongrg@seu.edu.cn

EXPERIMENTAL SECTION

Sample preparation. We first synthesized 2-trimethylammonioethylammonium dihydrochloride ([TMAEA]Cl_2). 2-Chloroethylamine hydrochloride (100 mmol) was completely dissolved in 100 mL ethanol and transferred to a single-necked round-bottomed flask containing a trimethylamine ethanol solution (120 mmol), and the single-necked round-bottomed flask was closed. The mixture was reacted at 343 K for 12 h, and a large amount of white precipitate was produced in the bottle after the reaction was finished. The precipitate was filtered and washed three times with ethanol to obtain a very pure white solid. The white solid was recrystallized from deionized water to obtain crystal samples of [TMAEA]Cl_2. The phase purity of [TMAEA]Cl_2 was confirmed by PXRD results (Figure S1). Then, [TMAEA]Cl_2 and $PbCl_2$ were dissolved in concentrated hydrochloric acid by a stoichiometric ratio 1:2. Colorless crystals of [TMAEA]Pb_2Cl_6 were finally obtained after a slow evaporation of the solvent. For the preparation of thin film sample of [TMAEA]Pb_2Cl_6, the precursor solution was prepared by dissolving 100 mg of the as-grown crystals of [TMAEA]Pb_2Cl_6 in 1 ml concentrated HCl aqueous solution. Spreading a drop of the precursor solution on the clean glass substrate and then annealing the substrate at 348 K obtain the thin film sample of [TMAEA]Pb_2Cl_6.

Characterization methods. We used the Rigaku D/MAX 2000 PC X-ray diffraction instrument in the 2θ between 5° and 50° with a step size of 0.02° to record PXRD patterns. Single-crystal X-ray diffraction data were performed using Mo-Kα radiation (λ = 0.71073) on a Rigaku Saturn 924 diffractometer in the ω scan mode. The crystal data were collected at 293 K, 393 K, and 423 K, respectively for [TMAEA]Pb_2Cl_6 and at 293 K for [TMAEA]Cl_2. We used the CrystalClear software

package to process the data. The crystal structures were solved by using the SHELXLTL software package. Differential scanning calorimetry (DSC) curves were recorded by using a NETZSCH DSC 200F3 instrument under a nitrogen atmosphere. The dielectric measurements were carried out on an automatic impedance Tonghui 2828 analyzer. For SHG experiments, an unexpanded laser beam with low divergence (pulsed Nd:YAG at a wavelength of 1064 nm, 5 ns pulse duration, 1.6 MW peak power, 10 Hz repetition rate) was used. The instrument model is Ins 1210058, INSTEC Instruments, while the laser is Vibrant 355 II, OPOTEK. The double-wave method for recording polarization−electric field hysteresis loops was carried out for thin film sample on a home-built system consisting of programmable waveform generator (Agilent, Model: 33521A), high voltage amplifier (Trek, Model: 623B) and programmable low-current electrometer (Keithley, Model: 6514). PFM visualization of the ferroelectric domain structures was carried out using a commercial atomic force microscope system (MFP-3D, Asylum Research). We used conductive Pt/Ir-coated silicon probes (EFM, Nanoworld) to study domain imaging and polarization switching with a resonant-enhanced PFM mode for enhancing the signal. Ultraviolet-vis (UV-vis) absorption spectra was measured with Shimadzu UV-2600 equipped with ISR-2600Plus integrating sphere.

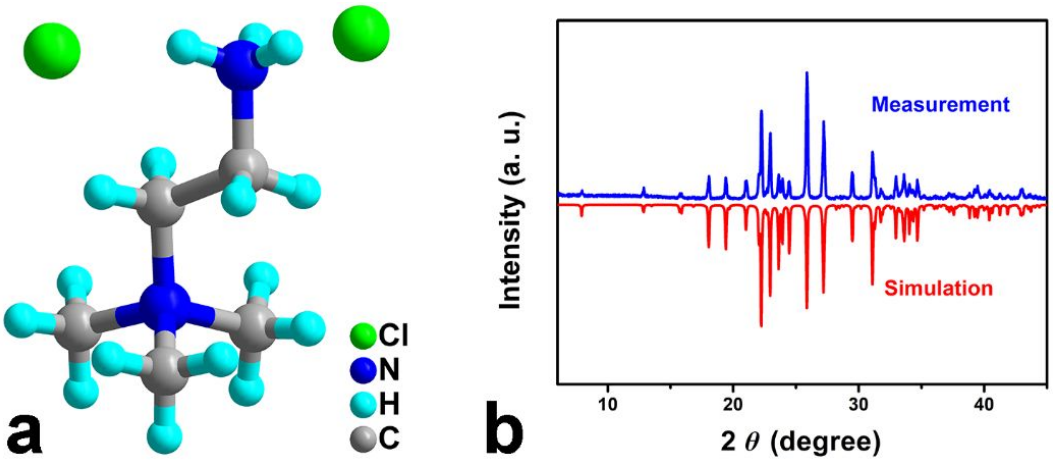

Figure S1. (a) Crystal structures of [TMAEA]Cl_2. [TMAEA]Cl_2 crystallizes in the triclinic space group $P\bar{1}$ with the unit cell lengths (a, b and c) of 5.68920(10), 7.09760(10) and 11.5466(3) Å and cell angles (α, β and γ) of 76.351(2), 82.677(2), 84.635(2)°. (b) PXRD patterns of as-prepared samples of [TMAEA]Cl_2, confirming the phase purtiy.

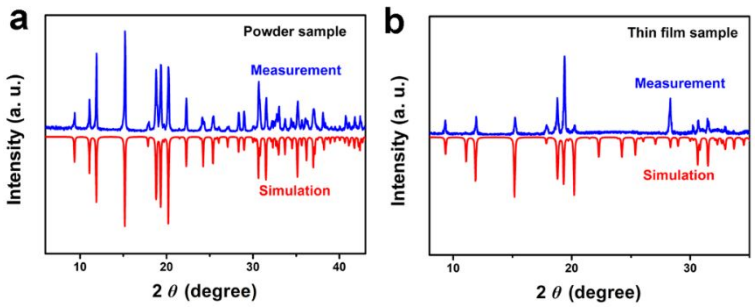

Figure S2. PXRD patterns of powder sample and thin film sample of [TMAEA]Pb_2Cl_6, verifying the phase purity.

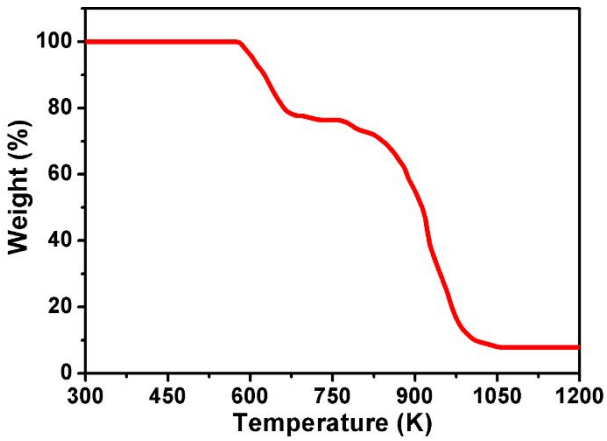

Figure S3. Thermogravimetric analysis (TGA) curves of [TMAEA]Pb_2Cl_6 recorded on a DAZHAN TGA-101 apparatus under air atmosphere, showing a good thermal stability up to about 580 K.

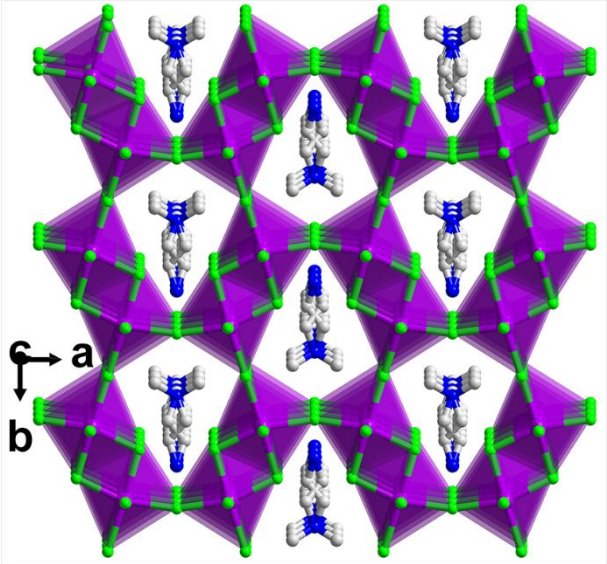

Figure S4. Crystal structures of [TMAEA]Pb_2Cl_6 at 293 K, showing that the $PbCl_6$ octahedron connects with an adjacent one through the edge-sharing mode to form a $[Pb_2Cl_6]^{2-}$ dimer, which further links with adjacent dimers through the corner-sharing mode to form a 3D network.

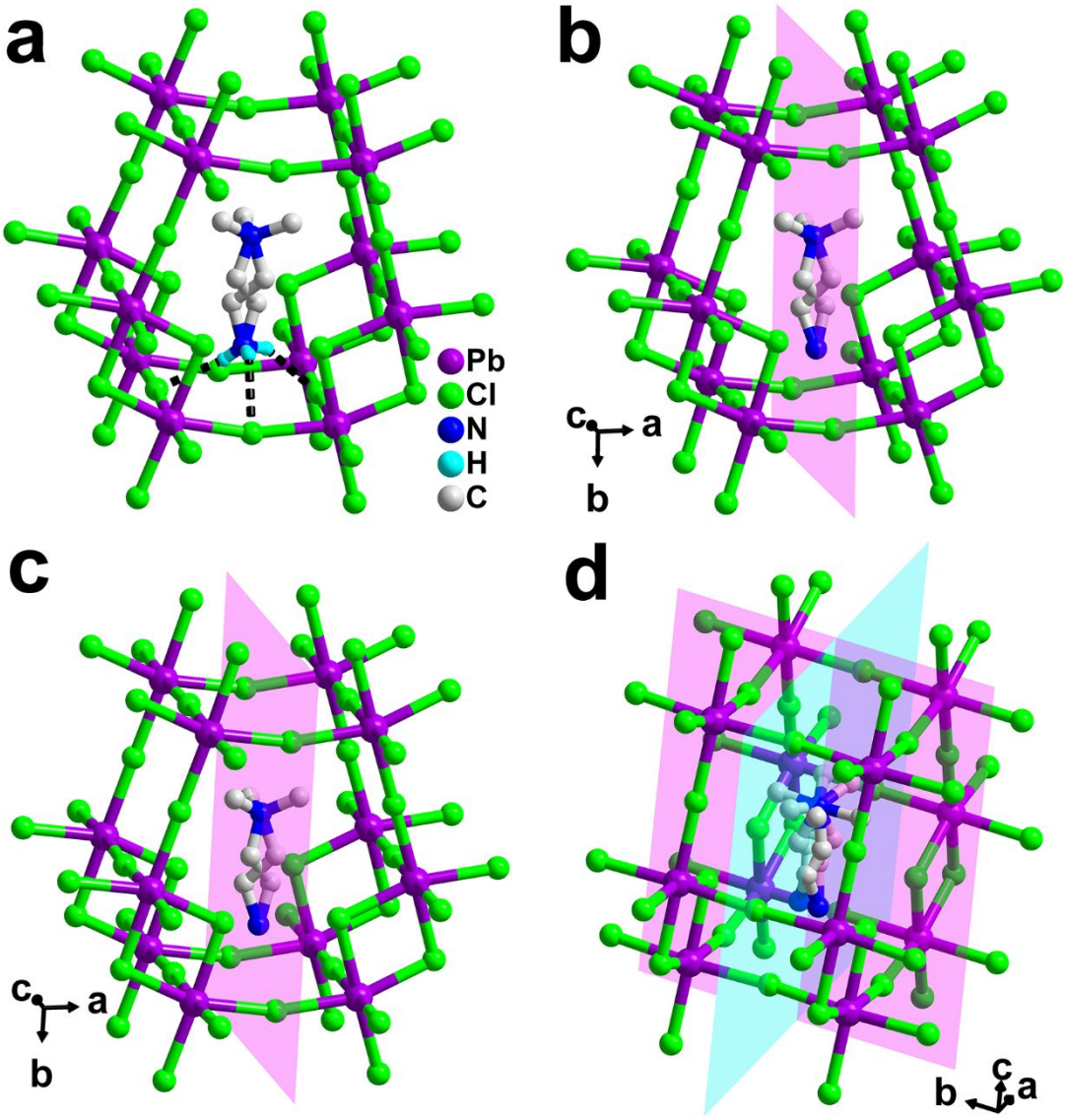

Figure S5. (a) Crystal structures of $[TMAEA]Pb_2Cl_6$ at 293 K, showing the N–H···Cl hydrogen-bonding interactions between the anionic framework and $[TMAEA]^+$ cations. (b) Crystal structures of $[TMAEA]Pb_2Cl_6$ at 293 K. $[TMAEA]^+$ cation is located on a symmetry position of a mirror plane parallel to the *bc* plane (pink plane). (c) Crystal structures of $[TMAEA]Pb_2Cl_6$ at 393 K. $[TMAEA]^+$ cation is also located on a symmetry position of a mirror plane parallel to the *bc* plane (pink plane). (d) Crystal structures of $[TMAEA]Pb_2Cl_6$ at 423 K. $[TMAEA]^+$ cation is located on a symmetry position of two mirror planes parallel to the *bc* plane (pink plane) and the *ac* plane (turquoise plane), respectively.

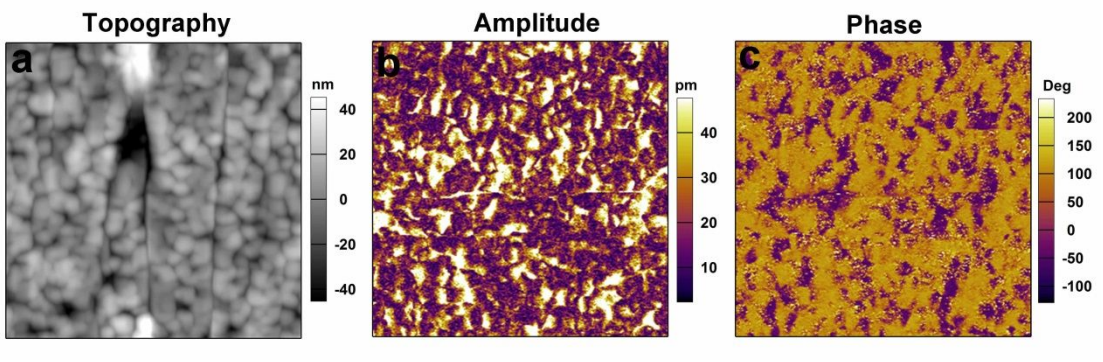

Figure S6. Vertical PFM imaging for the same region shown in Figure 3. (a) Topography, (b) PFM amplitude and (c) phase images.

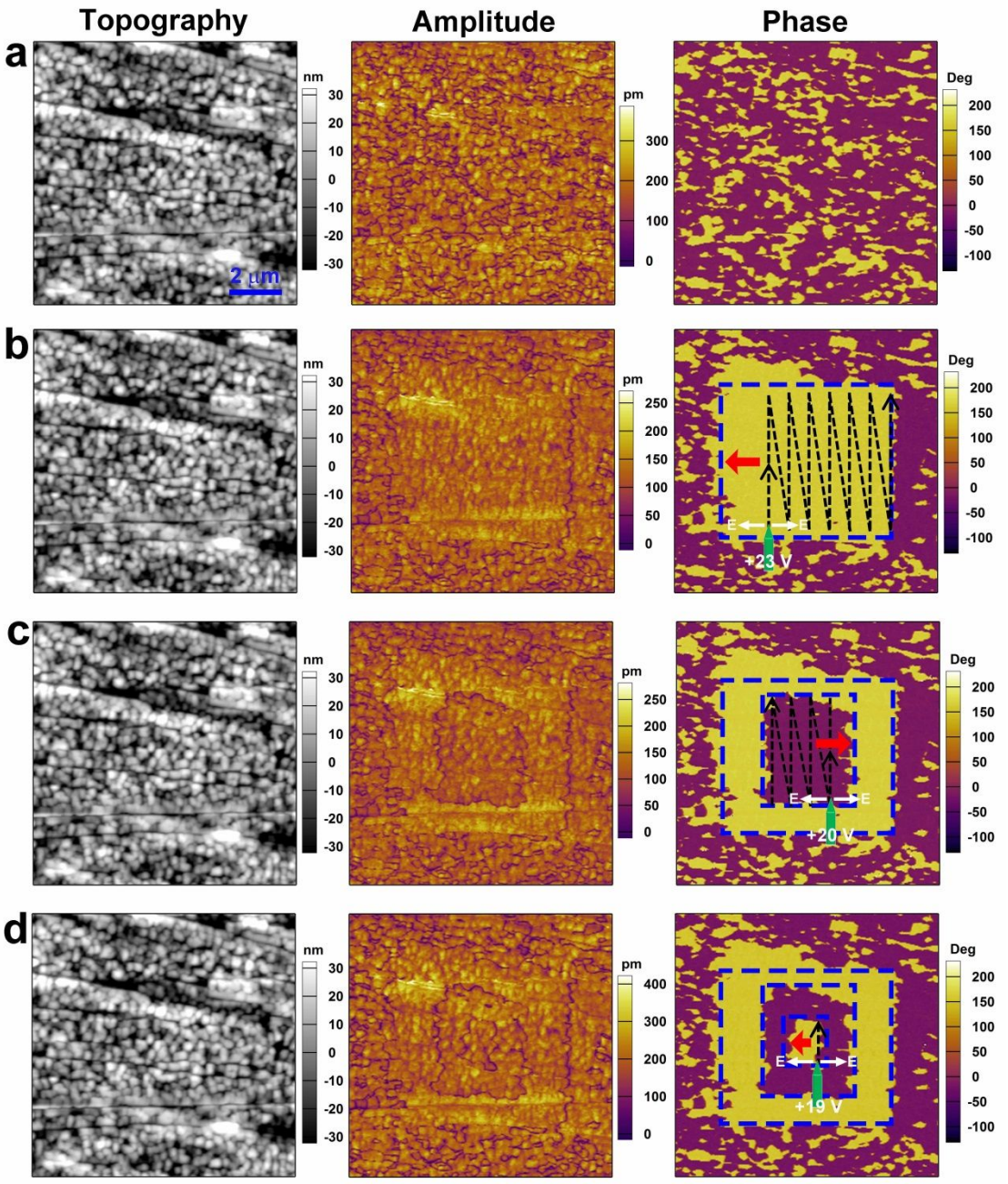

Figure S7. Domain switching experiments for [TMAEA]Pb_2Cl_6. Topography (left column), PFM amplitude (middle column) and PFM phase (right column) images for a selected region in [TMAEA]Pb_2Cl_6 thin film. (a) At pristine state, (b, c, d) three steps electric poling, which performed by moving the positively biased PFM tip along the dashed black lines in b, c, and d successively. The fat red arrows denote the trailing field.

The PFM measurements have been revealed that the polarization vector of the region in the [TMAEA]Pb_2Cl_6 thin film we have detected mainly lies in the in-plane direction. To control the in-plane domain switching, we move the biased PFM tip along a certain path. During the tip motion, it will create a net electric field vector at the rear side of the scan direction, the so-called trailing field.[1] The final polarization state of the domains will be aligned to the direction of the trailing field, and thus we can use this trailing field to write the domains determinately.

The initial mapping for a selected region shows a polydomain structure (Figure S7a). We then move the positively biased tip along the black dashed line in Figure S7b with voltage of +23 V and speed of 2 m/s. The direction of the trailing field is opposite to its movement. In this case, it is point to the left. From the resultant phase image (Figure S7b), we observed that the color tones of the central domains were became yellow, indicating a uniform polarization which should be aligned along the direction of the trailing field. Following domain reversal can be achieved by changing the moving path and thus changing the direction of trailing field. As shown in Figure S7c and d, the written domain can be further switched back and forth by moving the biased tip along the black dashed lines with voltages of +20 V and +19 V and speed of 2 m/s, successively. Finally, a box-in-box domain pattern can be generated. The domain walls can be clearly discerded in the corresponding amplitude images, where the signal is null. Meanwhile, there are no obvious changes in the corresponding surface morphologies. Therefore, our domain switching experiments confirmed the switchable polarization in [TMAEA]Pb_2Cl_6.

Reference:

(1) Sha, T.-T.; Xiong, Y.-A.; Pan, Q.; Chen, X.-G.; Song, X.-J.; Yao, J.; Miao, S.-R.; Jing, Z.-Y.; Feng, Z.-J.; You, Y.-M.; Xiong, R.-G. Fluorinated 2D Lead Iodide Perovskite Ferroelectrics. *Adv. Mater.* **2019**, *31*, 1901843

Table S1. Crystal data and structure refinements for [TMAEA]Pb_2Cl_6 at 293 K, 393 K, and 423 K, respectively.

Formula	$[(CH_3)_3NC_2H_4NH_3]Pb_2Cl_6$		
Temperature	293 K	393 K	423 K
Weight	731.30	731.30	731.30
Crystal system	Orthorhombic	Orthorhombic	Orthorhombic
Space group	*Pma*2	*Pma*2	Pmma
a/Å	14.8771 (9)	14.9094 (6)	14.9183 (9)
b/Å	9.4425 (5)	9.4872 (4)	5.8648 (3)
c/Å	5.8322 (4)	5.8622 (3)	9.4829 (5)
β/deg	90	90	90
Volume/Å^3	819.29 (9)	829.20 (6)	829.69 (8)
Z	2	2	2
*R*1 [$I>2\sigma(I)$]	0.0545	0.0358	0.0494
*wR*2 [$I>2\sigma(I)$]	0.1520	0.0910	0.1422
GOF	1.003	1.004	1.008

Table S2. Selected Cl−Pb bond lengths [Å] and Cl−Pb−Cl bond angles [°] for [TMAEA]Pb_2Cl_6 at 293 K, 393 K, and 423 K, respectively.

Temperature	bond lengths [Å]		bond angles [°]	
293 K	Pb1—Cl2	2.81 (4)	Cl2—Pb1—Cl3^{i}	92.4 (6)
	Pb1—Cl3^{i}	2.841 (8)	Cl2—Pb1—Cl1	93.9 (10)
	Pb1—Cl1	2.863 (2)	Cl3^{i}—Pb1—Cl1	97.74 (15)
	Pb1—Cl4	2.875 (2)	Cl2—Pb1—Cl4	87.2 (9)
	Pb1—Cl3	2.886 (7)	Cl3^{i}—Pb1—Cl4	162.5 (3)
	Pb1—Cl2^{ii}	3.02 (4)	Cl1—Pb1—Cl4	99.8 (3)
	Cl1—Pb1^{iii}	2.864 (2)	Cl2—Pb1—Cl3	89.9 (6)
	Cl2—Pb1^{iv}	3.02 (4)	Cl3^{i}—Pb1—Cl3	80.8 (2)
	Cl3—Pb1^{i}	2.841 (8)	Cl1—Pb1—Cl3	176.0 (11)
	Cl4—Pb1^{v}	2.875 (2)	Cl4—Pb1—Cl3	81.6 (3)
			Cl2—Pb1—Cl2^{ii}	176.2 (4)
			Cl3^{i}—Pb1—Cl2^{ii}	89.4 (6)
			Cl1—Pb1—Cl2^{ii}	89.1 (10)
			Cl4—Pb1—Cl2^{ii}	90.1 (8)
			Cl3—Pb1—Cl2^{ii}	87.1 (6)
			Pb1—Cl1—Pb1^{iii}	175.3 (19)
			Pb1—Cl2—Pb1^{iv}	176.2 (4)

			$Pb1^{i}$—Cl3—Pb1	99.1 (2)
			Pb1—Cl4—$Pb1^{v}$	163.7 (6)
393 K	Pb1—$Cl3^{i}$	2.860 (4)	$Cl3^{i}$—Pb1—Cl1	97.91 (7)
	Pb1—Cl1	2.8714 (6)	$Cl3^{i}$—Pb1—Cl4	162.09 (14)
	Pb1—Cl4	2.8769 (10)	Cl1—Pb1—Cl4	99.99 (14)
	Pb1—Cl3	2.898 (3)	$Cl3^{i}$—Pb1—Cl3	80.78 (11)
	Pb1—$Cl2^{ii}$	2.93 (3)	Cl1—Pb1—Cl3	178.1 (6)
	Pb1—Cl2	2.94 (3)	Cl4—Pb1—Cl3	81.32 (15)
	Cl1—$Pb1^{iii}$	2.8714 (6)	$Cl3^{i}$—Pb1—$Cl2^{ii}$	91.5 (4)
	Cl2—$Pb1^{iv}$	2.93 (3)	Cl1—Pb1—$Cl2^{ii}$	92.6 (7)
	Cl3—$Pb1^{i}$	2.860 (4)	Cl4—Pb1—$Cl2^{ii}$	88.5 (7)
	Cl4—$Pb1^{v}$	2.8769 (10)	Cl3—Pb1—$Cl2^{ii}$	88.9 (3)
			$Cl3^{i}$—Pb1—Cl2	90.3 (3)
			Cl1—Pb1—Cl2	90.9 (7)
			Cl4—Pb1—Cl2	88.7 (7)
			Cl3—Pb1—Cl2	87.7 (3)
			$Cl2^{ii}$—Pb1—Cl2	175.9 (2)
			Pb1—Cl1—$Pb1^{iii}$	178.3 (14)
			$Pb1^{iv}$—Cl2—Pb1	175.9 (2)
			$Pb1^{i}$—Cl3—Pb1	99.21 (10)
			$Pb1^{v}$—Cl4—Pb1	164.4 (3)
423 K	Pb1—Cl4	2.843 (4)	Cl4—Pb1—Cl2	98.03 (8)
	Pb1—Cl2	2.8700 (5)	Cl4—Pb1—Cl3	161.76 (19)
	Pb1—Cl3	2.8763 (13)	Cl2—Pb1—Cl3	100.21 (17)
	Pb1—$Cl4^{i}$	2.892 (4)	Cl4—Pb1—$Cl4^{i}$	80.21 (11)
	Pb1—$Cl1^{ii}$	2.9341 (3)	Cl2—Pb1—$Cl4^{i}$	178.24 (8)
	Pb1—Cl1	2.9341 (3)	Cl3—Pb1—$Cl4^{i}$	81.54 (18)
	Cl1—$Pb1^{iii}$	2.9341 (2)	Cl4—Pb1—$Cl1^{ii}$	90.81 (11)
	Cl2—$Pb1^{iv}$	2.8701 (5)	Cl2—Pb1—$Cl1^{ii}$	91.67 (11)
	Cl3—$Pb1^{v}$	2.8763 (13)	Cl3—Pb1—$Cl1^{ii}$	88.67 (11)
	Cl4—$Pb1^{i}$	2.892 (4)	$Cl4^{i}$—Pb1—$Cl1^{ii}$	88.37 (11)

Cl4—Pb1—Cl1	90.81 (11)
Cl2—Pb1—Cl1	91.67 (11)
Cl3—Pb1—Cl1	88.67 (11)
Cl4^{i}—Pb1—Cl1	88.37 (11)
Cl1^{ii}—Pb1—Cl1	176.1 (2)
Pb1^{iii}—Cl1—Pb1	176.1 (2)
Pb1—Cl2—Pb1^{iv}	180.0
Pb1—Cl3—Pb1^{v}	164.8 (3)
Pb1—Cl4—Pb1^{i}	99.78 (11)

Symmetry code(s):

293 K: (i) −*x*, −*y*+1, *z*; (ii) *x*, *y*, *z*−1; (iii) −*x*, −*y*+2, *z*; (iv) *x*, *y*, *z*+1; (v) −*x*+1/2, *y*, *z*.

393 K: (i) −*x*, −*y*+1, *z*; (ii) *x*, *y*, *z*−1; (iii) −*x*, −*y*+2, *z*; (iv) *x*, *y*, *z*+1; (v) −*x*+1/2, *y*, *z*.

423 K: (i) −*x*+1, −*y*+1, −*z*+2; (ii) *x*, *y*−1, *z*; (iii) *x*, *y*+1, *z*; (iv) −*x*+1, −*y*+1, −*z*+1; (v) −*x*+1/2, −*y*+1, *z*; (vi) −*x*+3/2, −*y*+2, *z*; (vii) −*x*+3/2, *y*, *z*; (viii) *x*, −*y*+2, *z*.